ELSEVIER

Nuclear Instruments and Methods in Physics Research B 161–163 (2000) 308–313

NIM B
Beam Interactions with Materials & Atoms

www.elsevier.nl/locate/nimb

Simultaneous and consistent analysis of NRA, RBS and ERDA data with the IBA DataFurnace

N.P. Barradas [a,*,1], S. Parascandola [b], B.J. Sealy [a], R. Grötzschel [b], U. Kreissig [b]

[a] *School of Electronic Engineering, Information Technology and Mathematics, University of Surrey, Guildford, Surrey GU2 5XH, UK*
[b] *Forschungszentrum Rossendorf e.V., Postfach 510119, 01314 Dresden, Germany*

Abstract

We present in this paper, for the first time, the extension of the ion beam analysis DataFurnace to the analysis of non-resonant nuclear reaction analysis (NRA) data. The NRA routine is general and can be used to analyse data from any reaction with known Q and cross section. The shape of the cross section is taken into account and hence depth profiling using reactions with non-flat cross sections is easily done. We show different applications of the program, including profiling of deuterium with a ^{3}He beam and profiling of N in a stainless steel matrix using a deuterium beam. In the latter case, we also performed 35 MeV Cl-ERDA and D-RBS experiments of the same sample. The Ion Beam Analysis DataFurnace allows to analyse all the data simultaneously, taking into account all the information present in the different data sets in a fully consistent manner. © 2000 Published by Elsevier Science B.V. All rights reserved.

PACS: 82.80.Yc; 07.05.Kf; 02.60.Ed; 02.70.Lq
Keywords: NRA; RBS; ERDA; Data analysis; Simulated annealing

1. Introduction

The ion beam analysis DataFurnace (NDF) [1,2] is a computer program that utilises the simulated annealing algorithm (SA) [3,4] to analyse ion beam analysis data in an automated way, with minimum human intervention. The user must only input the data, the experimental conditions and the elements present in the sample, with no interactive simulation procedure involved. While in the past NDF was limited to the analysis of RBS and ERDA data it has been extended recently to the analysis of non-resonant Nuclear Reaction Analysis data. We show two applications of the new NRA data routine, including the simultaneous and self-consistent analysis of NRA, RBS and ERDA spectra collected from the same sample.

2. Experimental details

The Surrey 2 MV van de Graaff [5] was used to produce a 0.7 MeV $^3He^+$ beam, employed to profile deuterium in multilayered deuterated polystyrene

* Corresponding author. Tel.: +44-1483-259-823; fax: +44-1483-534-139.
E-mail address: n.barradas@surrey.ac.uk (N.P. Barradas).
[1] Present address: Instituto Tecnológico e Nuclear, E.N. 10, 2685 Sacavém, Portugal.

0168-583X/00/$ - see front matter © 2000 Published by Elsevier Science B.V. All rights reserved.
PII: S 0 1 6 8 - 5 8 3 X (9 9) 0 0 9 7 6 - 3

(PS, with chemical composition CH) with nominal structure d-PS 32.3 nm/PS 63.3 nm/d-PS 32.3 nm/bulk PS, taking advantage of the reaction d(^{3}He, p)^{4}He with $Q = 18.352$ MeV. The known cross section values [6,7], which change rapidly with beam energy, were used. Grazing angles of incidence between $\alpha = 2°$ and $\alpha = 10°$ were used to improve the depth resolution, where α is the angle between the beam and the sample surface. Two detectors were used, at angles of $\varphi = 165°$ and $\varphi = 180°$ (annular detector) with the beam, with resolution 15 and 70 keV at FWHM respectively.

Austenitic stainless steel (AISI 321, $Cr_{18}Fe_{65}Ni_{12}$) has been nitrided for 4 h at 380°C by plasma immersion ion implantation (PIII). High voltage pulses of 5 kV amplitude were applied at a repetition rate of 1100 Hz. The sample was measured at Rossendorf [8] with NRA, RBS and ERDA. A 1.4 MeV d^+ beam (with a smaller than 5% H_2^+ contamination) was used for the NRA and RBS experiments. The resulting spectrum is complex, including contributions from the recoils and different reactions. The reaction $^{14}N(d,\alpha_1)^{12}C$ with $Q = 9.146$ MeV was used to profile the nitrogen while the backscattered (d-RBS) spectrum was used for the metal matrix. The cross section values of the nuclear reaction were obtained from [9]. The detector was located at $\varphi = 170°$ with the beam and had a 17 keV resolution. Normal incidence was used. Two different ERDA experiments were done. In both cases a 35 MeV $^{35}Cl^{7+}$ beam was used. An angle-resolving ionisation chamber which can be used for in situ real-time depth profiling (ARIC-ERDA) [10], with an active length of 280 mm filled with 38 mbar isobutane detector with 330 keV resolution was located at $\varphi = 35°$. The angle of incidence was $\alpha = 17.5°$. A 1.5 μm thick mylar ($C_{10}H_8O_4$) foil was located before the detector. Time-of-flight ERDA experiments were carried out at $\varphi = 45°$ and $\alpha = 22.5°$, with a 284 keV resolution. A 60 nm thick C foil was located before the detector.

3. Spectrum synthesis, fitting and profiling

Synthesis of RBS and ERDA spectra is standard and well documented (see [11] for a review and [12] for an alternative efficient method). They are normally based on variations of the relationship [11,13,14]

$$Y_j(E^{\mathrm{det}}_{j:j+1}) = \mathrm{Q}\Omega(Nt)_{j:j+1}\ \sigma(E^{\mathrm{in}}_{j:j+1})/\cos(90° - \alpha), \tag{1}$$

where Y_j is the yield in channel j due to one isotope, $E^{\mathrm{det}}_{j:j+1}$ is the range of detected energies corresponding to channel j $(Nt)_j$ is the areal density in a layer which generates detected particles with energies in the $E^{\mathrm{det}}_{j:j+1}$ range, $E^{\mathrm{in}}_{j:j+1}$ is the beam energy before interaction, $\sigma(E^{\mathrm{in}}_{j:j+1})$ is the cross section, α is the angle of incidence, and $\mathrm{Q}\Omega$ is the charge–solid angle product. Most codes divide the sample in slabs of constant concentration and tabulate $(Nt)_k$, E^{in}_k and E^{det}_k values corresponding to slab k. Y_j is then calculated for all channels j, using $E^{\mathrm{det}}_{j:j+1}$ as reference to interpolate $(Nt)_{j:j+1}$ and $E^{\mathrm{in}}_{j:j+1}$ in Eq. (1) from those tables. Finally one adds all the partial spectra corresponding to each isotope and each element to form the final spectrum.

Although Eq. (1) is also valid for NRA, the method described above is not generally valid to synthesise NRA spectra. In RBS and ERDA $E^{\mathrm{det}}_{j:j+1}$ changes monotonically (it actually decreases) with depth, such that each channel can be assigned to a well defined depth range, that is, a well defined $E^{\mathrm{in}}_{j:j+1}$. In NRA it may decrease or increase, depending on the exact reaction and stopping power values involved. In some cases, such as the reaction $^{11}B(p,^4He)^8B$ with $Q = 5.650$ MeV at proton energies below 200 keV, $E^{\mathrm{det}}_{j:j+1}$ is not a monotonic function of E^{in} and different depth ranges can contribute to the same channel. In this case the interpolations described above fail. To generate the spectrum one must proceed not from channel to channel but from slab to slab. Slab k will in general correspond to several channels $j_1, \ldots, j_n$ (including fractions of channel at the borders) and one calculates $Y_{j1}, \ldots, Y_{jn}$ for all. Different slabs may contribute to the same channel. This process is cumbersome and time-consuming, but it is general, and is implemented in NDF for NRA.

Algorithms to calculate apparent depth profiles that follow the data point by point have been presented for RBS [15] and ERDA [16]. The stopping powers can be calculated in an iterative

way, directly from the data, which makes the procedure self-consistent and fully automatic, but requires that the signals corresponding to all elements except one must be present and separated from each other, which is not always the case. In the widely used RUMP code [13] the stopping powers are calculated from a rough user-defined structure. In this case, the signal from the element under consideration must be fully separated, but the signals from the other elements present are not required. In NDF a similar algorithm is implemented, but it uses the fact that the SA fit effectively separates the signals of the different elements [17]. Point by point profiles, that is $(Nt)_{j:j+1}$, are thus automatically calculated at the end of the fit for all elements for which a signal is detected, by using Eq. (1) with the E_k^{in} and E_k^{det} values calculated for the best fit and taking Y_j to be the data. This is also done for NRA when possible, that is, when $E_{j:j+1}^{\mathrm{det}}$ is a monotonic function of E_{in}. The results are only as good as the SA fit, as they rely on the fit for signal separation and stopping power calculation.

4. Results and discussion

The proton spectra obtained for the d-PS 32.3 nm/PS 63.3 nm/d-PS 32.3 nm/bulk PS, sample with the d(^{3}He,p)^{4}He reaction are shown in Fig. 1.

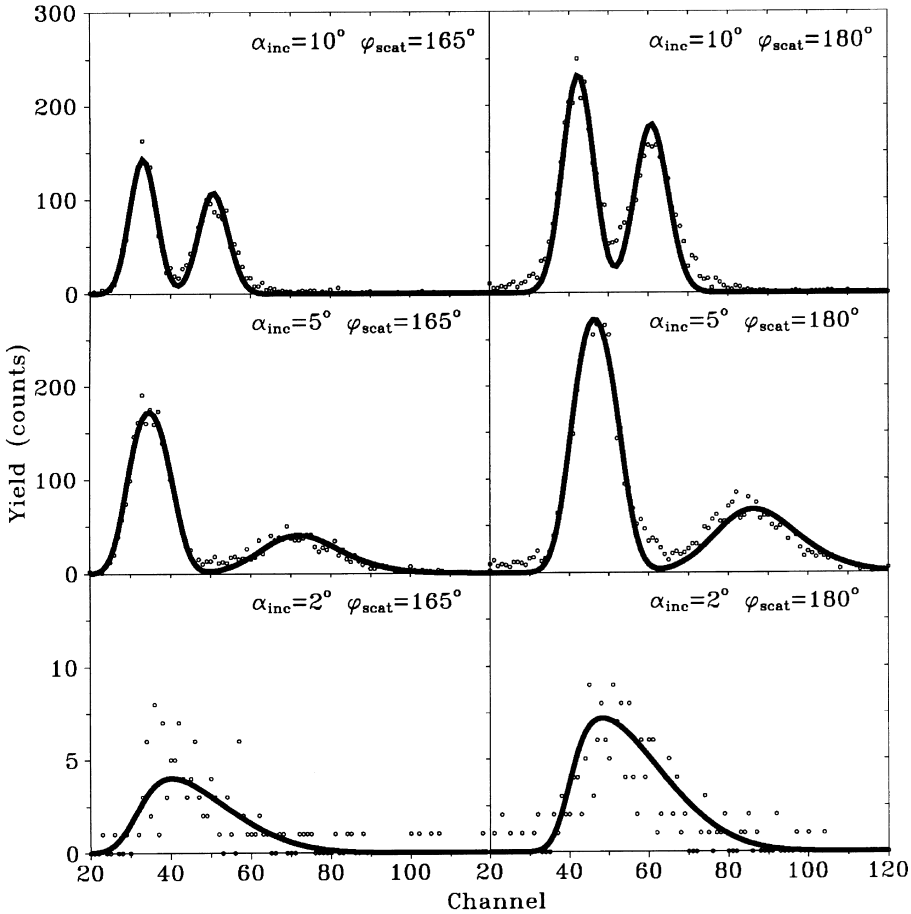

Fig. 1. NRA spectra (dots) and fit (solid line) for the d-PS 32.3 nm/PS 63.3 nm/d-PS 32.3 nm/bulk PS sample with the d(^{3}He,p)^{4}He reaction.

Note that the observed energy increases monotonically with depth. All data were fitted simultaneously with the same depth profile. A single peak is observed at $\alpha = 2°$ because in that case the ^{3}He particles lose all their energy before they reach the second d-PS layer.

The shape of the spectra is strongly affected by the fast degradation of the energy resolution with depth, which at such grazing angles is dominated by multiple scattering of the ^{3}He beam (the multiple scattering of the p particles on the way out is much smaller due to the smaller Z). We have used the DEPTH code [18] to calculate the energy resolution as a function of depth for the different experimental geometries used. The values obtained were integrated in the fit using the method given in Ref. [19], ensuring that the spectral shape could be correctly reproduced without broadening of the depth profile obtained. That all spectra could be fitted with the same depth profile demonstrates the consistency of the method.

The final fitted layer structure was d-PS 38.4 nm/PS 69.9 nm/d-PS 32.4 nm/bulk PS, with sharp interfaces between the layers, in good agreement with the nominal structure. It is shown in Fig. 2 for deuterium. The point by point apparent profiles are also shown. They are much broader than the fitted structure, because the effects of energy resolution due to broadening are not taken into account in their calculation. Further, the results for the spectra taken at $\alpha = 2°$ (triangles and crosses in Fig. 2) show a very large scattering due to the low statistics of the data.

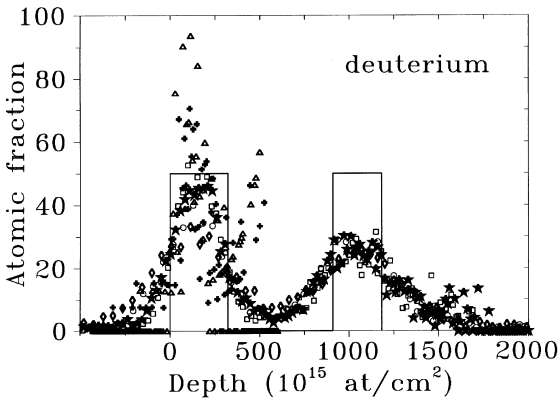

Fig. 2. Deuterium fitted depth profile (solid line) obtained for a multilayered deuterated polystyrene sample. Apparent depth profiles calculated from the data are also shown. Each point type corresponds to a different spectrum.

The ERDA, NRA and d-RBS spectra obtained for a nitrided austenitic stainless steel are shown in Fig. 3. The first observation is that the spectra are complementary, as each one provides different information. The in situ ERDA experiment has good depth resolution at the surface of the sample due to the grazing angle of incidence and shows an increased N concentration in a thin surface layer, but the probed depth is small. The depth resolution of the TOF-ERDA experiment is slightly worse, but a deeper depth can be probed. With the NRA experiment the full N profile can be probed, but at the cost of a poor depth resolution. Finally, the d-RBS experiment provides direct information on the metal signal.

We did not include DEPTH [18] calculations on the fits because the data do not have marked fast-changing features. This leads however to the step structure of the fit to the NRA data, where each step corresponds to one layer of equal concentration as determined during the fit. Including full calculations of the energy resolution as a function of depth would lead to a smooth fitted curve, at the expense of increasing calculation time.

The shape difference between the fitted function and the data in the RBS spectrum below channel 150 is due either to the effect of plural scattering [20] or to incorrect stopping power values. In fact, to obtain a simultaneous good fit to the width of the NRA N signal and to the width of the d-RBS metal signal we had to scale down the deuterium stopping powers by 5%. This was a constant factor in all the energy range, while a change in the energy dependence of the stopping powers would also lead to a change in the shape of the fitted spectrum as well.

Fitting simultaneously all spectra ensures that all the information in the different spectra is taken into account during the fit and is incorporated in the final solution obtained. The final fitted depth profile is shown in Fig. 4. It combines the features given by the four spectra, with an increased N concentration at the very surface. This is followed by a slow concentration decrease towards the bulk

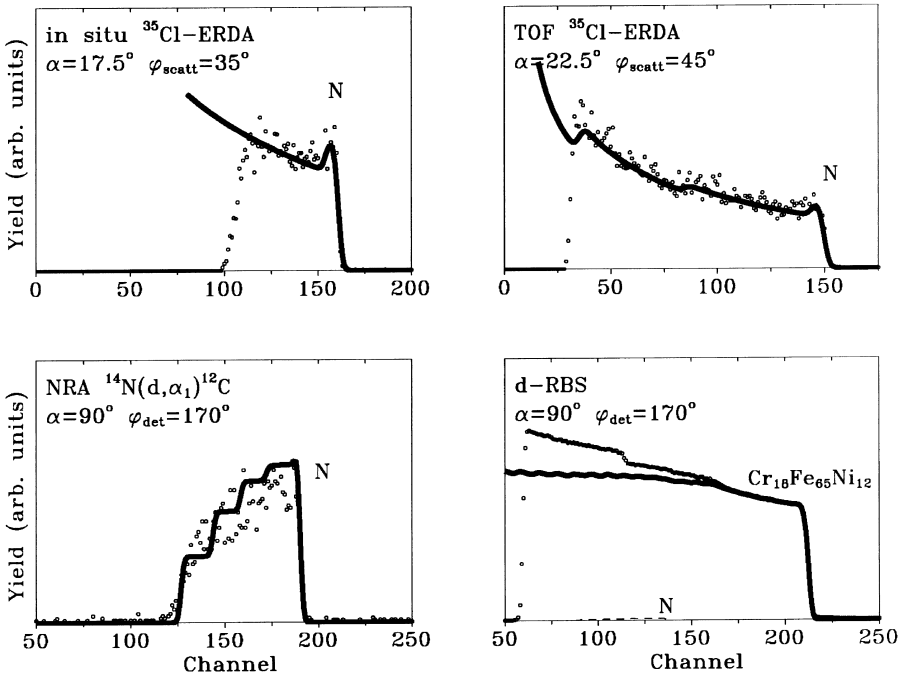

Fig. 3. In situ ERDA, Time-of-flight (TOF) ERDA, NRA and d-RBS spectra (dots) obtained for a nitrided austenitic stainless steel and corresponding fits (solid lines). The step observed at channel 115 on the d-RBS spectrum is due to a H_2^+ beam contamination. The NRA and RBS spectra have been shifted towards low channel numbers.

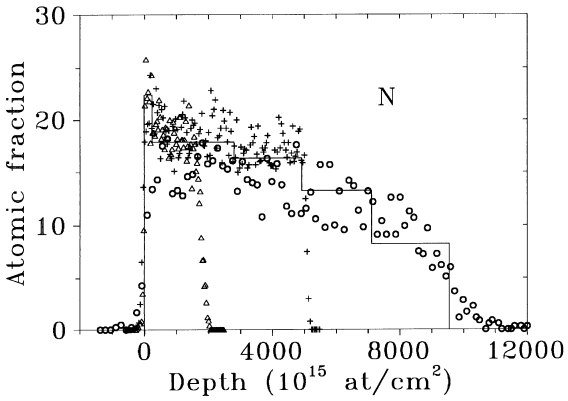

Fig. 4. Fitted depth profile obtained for a nitrided austenitic stainless steel (solid line). Point by point N profiles calculated from the in situ ERDA (triangles), TOF-ERDA (crosses) and NRA (circles) data are also shown.

of the sample. The calculated apparent N depth profiles are also shown for the ERDA and NRA data, but not for the RBS data where sensitivity to N is minimal. Note that for the ERDA experiments the apparent profiles end abruptly, which simply reflects the limited probed depth in those experiments.

5. Summary

- The IBA DataFurnace was extended to fit NRA data. The code written is general and can handle any reaction with known Q and known cross sections.
- A routine to make a direct conversion of NRA data into apparent depth profiles was also written. It can handle all reactions where the detected energy is a monotonic function of the beam energy before interaction.
- The code was succesfully applied to the profiling of deuterium using a ^{3}He beam at grazing angle of incidence. In this case the degradation

of energy resolution with depth must be taken into account for a correct evaluation of the data.

- The code was also successfully applied to the consistent analysis of NRA, RBS and ERDA data collected from a nitrided austenitic stainless steel sample. All information present in the complementary spectra is taken into account in the derivation of the depth profile, that then reflects all features in the data.

Acknowledgements

NPB would like to thank Dr. Chris Jeynes for his critical reading of the manuscript, and R. Smith and Dr. A.S. Clough for the ^{3}He experiments. This work was carried out under EPSRC contract GRL78512 and the EU Large Scale Facility grant FMGE-CT98-0146.

References

[1] N.P. Barradas, C. Jeynes, R.P. Webb, Appl. Phys. Lett. 71 (1997) 291.
[2] N.P. Barradas, C. Jeynes, R.P. Webb, U. Kreissig, R. Grötzschel, Nucl. Instr. and Meth. B 149 (1999) 233.
[3] S. Kirkpatrick, C.D. Gelatt, M.P. Vecchi, Science 220 (1983) 671.
[4] E. Aarts, J. Korst, Simulated Annealing and Boltzmann Machines: A Stochastic Approach to Combinatorial Optimization and Neural Computing, Wiley, Chichester, 1989.
[5] C. Jeynes, N.P. Barradas, M.J. Blewett, R.P. Webb, Nucl. Instr. and Meth. B 136–138 (1998) 1229.
[6] C.J. Altstetter, R. Behrisch, J. Bøttiger, F. Pohl, B.M.U. Scherzer, Nucl. Instr. and Meth. 149 (1978) 59.
[7] W. Möller, F. Besenbacher, Nucl. Instr. and Meth. 168 (1980) 111.
[8] U. Kreissig, S. Grigull, K. Lange, P. Nitzsche, B. Schmidt, Nucl. Instr. and Meth. B 136–138 (1998) 674.
[9] R.A. Jarjis, Nuclear Cross Section Data for Surface Analysis, vol. 3, Department of Physics, Schuster Laboratory, University of Manchester, 1979, p. 85.
[10] W. Assmann, H. Huber, C. Steinhausen, M. Dobler, H. Glückner, A. Weidinger, Nucl. Instr. and Meth. B 89 (1994) 131.
[11] E. Kótai, Nucl. Instr. and Meth. B 85 (1994) 588.
[12] Y. Serruys, Nucl. Instr. and Meth. B 61 (1991) 221.
[13] L.R. Doolittle, Nucl. Instr. and Meth. B 9 (1985) 291.
[14] G. Vizkelethy, Nucl. Instr. and Meth. B 45 (1990) 1.
[15] P. Børgesen, R. Behrisch, B.M.U. Scherzer, Appl. Phys. A 27 (1982) 183.
[16] C. Späth, F. Richter, S. Grigull, U. Kreissig, Nucl. Instr. and Meth. B 140 (1998) 243.
[17] N.P. Barradas, C. Jeynes, K.P. Homewood, B.J. Sealy, M. Milosavljevic, Nucl. Instr. and Meth. B 139 (1998) 235.
[18] E. Szilágyi, F. Pászti, G. Amsel, Nucl. Instr. and Meth. B 100 (1995) 103.
[19] N.P. Barradas, A.P. Knights, C. Jeynes, O.A. Mironov, T. Grasby, E.H.C. Parker, Phys. Rev. B 59 (1999) 5097.
[20] P. Bauer, E. Steinbauer, J.P. Biersack, Nucl. Instr. and Meth. B 64 (1992) 711.